Author Manuscript

Author Manuscript

Author Manuscript

Author Manuscript

HHS Public Access

Author manuscript

Stress. Author manuscript; available in PMC 2021 March 01.

Published in final edited form as:

Stress. 2020 March ; 23(2): 125–135. doi:10.1080/10253890.2019.1641081.

Myocardial Fibrosis, Inflammation, and Altered Cardiac Gene Expression Profiles in Rats Exposed to a Predator-Based Model of Posttraumatic Stress Disorder

Boyd R. Rorabaugh, Ph.D.[a,*], **Nathaniel W. Mabe, Pharm. D.**[b], **Sarah L. Seeley, B.S.**[a], **Thorne S. Stoops**[a], **Kasey E. Mucher**[c], **Connor P. Ney**[c], **Cassandra S. Goodman**[c], **Brooke J. Hertenstein**[c], **Austen E. Rush**[c], **Charis D. Kasler**[c], **Aaron M. Sargeant, Ph.D., D.V.M**[d], **Phillip R. Zoladz, Ph.D**[c]

[a]Department of Pharmaceutical and Biomedical Sciences, College of Pharmacy, Ohio Northern University, Ada, Ohio 45810 USA

[b]Department of Pharmacology and Cancer Biology, Duke University, Durham, North Carolina, USA

[c]Department of Psychology, Sociology, & Criminal Justice, Ohio Northern University, Ada, OH, USA

[d]Charles River Laboratories, Spencerville, Ohio, USA

Abstract

People who are exposed to life-threatening trauma are at risk of developing posttraumatic stress disorder (PTSD). In addition to psychological manifestations, PTSD is associated with an increased risk of myocardial infarction, arrhythmias, hypertension, and other cardiovascular problems. We previously reported that rats exposed to a predator-based model of PTSD develop myocardial hypersensitivity to ischemic injury. The present study characterized cardiac changes in histology and gene expression in rats exposed this model. Male rats were subjected to two cat exposures (separated by a period of 10 days) and daily cage-mate changes for 31 days. Control rats were not exposed to the cat or cage-mate changes. Ventricular tissue was analyzed by RNA sequencing, western blotting, histology, and immunohistochemistry. Multifocal lesions characterized by necrosis, mononuclear cell infiltration, and collagen deposition were observed in hearts from all stressed rats but none of the control rats. Gene expression analysis identified clusters of upregulated genes associated with endothelial to mesenchymal transition, endothelial migration, mesenchyme differentiation, and extracellular matrix remodeling in hearts from stressed rats. Consistent with endothelial to mesenchymal transition, rats from stressed hearts exhibited increased expression of α-smooth muscle actin (a myofibroblast marker) and a decrease in the number of CD31 positive endothelial cells. These data provide evidence that predator-based stress induces myocardial lesions and reprogramming of cardiac gene expression. These changes may underlie the myocardial hypersensitivity to ischemia observed in these animals. This rat

[*]Correspondence: Department of Pharmaceutical and Biomedical Sciences, College of Pharmacy, Ohio Northern University, 525 South Main Street, Ada, OH, 45810 USA; Telephone: 419-772-1695; Fax:419-772-1917; b-rorabaugh@onu.edu.

Author Manuscript Author Manuscript Author Manuscript Author Manuscript

model may provide a useful tool for investigating the cardiac impact of PTSD and other forms of chronic psychological stress.

Lay Summary

Chronic predator stress induces the formation of myocardial lesions characterized by necrosis, collagen deposition, and mononuclear cell infiltration. This is accompanied by changes in gene expression and histology that are indicative of cardiac remodeling. These changes may underlie the increased risk of arrhythmias, myocardial infarction, and other cardiac pathologies in people who have post-traumatic stress disorders or other forms of chronic stress.

Keywords

Posttraumatic stress disorder; stress; heart; predator stress; cardiac remodeling; cardiovascular

Introduction

Posttraumatic stress disorder (PTSD) is a disabling mental health disorder that develops following wartime combat, assault, rape, motor vehicle accidents, terrorist attacks, and other traumatic experiences. People with PTSD experience psychological distress by repeatedly reliving their trauma through intrusive flashback memories (Ehlers et al., 2002; Ehlers et al., 2004; Reynolds and Brewin, 1999). This is accompanied by debilitating symptoms such as nightmares, emotional numbing, avoidance of stimuli associated with the trauma, and persistent arousal and hypervigilance (Nemeroff et al., 2006; Pitman et al., 2012; Zoladz and Diamond, 2013).

In addition to psychological manifestations, PTSD is also associated with cardiovascular abnormalities including hypertension, increased risk of cardiac arrhythmias, atherosclerosis, and increased risk of myocardial infarction (Ahmadi et al., 2011; Beristianos et al., 2016; Khazaie et al., 2013; Vaccarino et al., 2013). However, little is known about the mechanisms that underlie the increased risk of cardiovascular disease in PTSD patients. The direct impact of PTSD on the heart is difficult to study in humans because PTSD is associated with increased rates of smoking, sedentary lifestyle, diabetes, depression, and other factors that influence cardiovascular function and potentially confound efforts to assess the direct impact of posttraumatic stress on the heart (Dedert et al., 2010; Zen et al., 2012). Animal models provide a tool to examine the impact of posttraumatic stress on the heart in the absence of these confounding variables.

Cat exposure is a well described and ethologically relevant stressor that produces an intense fear response in rats (Blanchard et al., 2003; Hubbard et al., 2004; Wilson et al., 2013; Wilson et al., 2014a; Wilson et al., 2014b). Our laboratory uses a cat-based model of psychosocial stress that incorporates features that are known to promote the development of PTSD including acute intense stress (predator exposure), lack of control over the stress (immobilization during predator exposure), a lack of social support (daily cage mate changes), and a re-experiencing of the stressful event (second predator exposure). Exposure to this animal model results in physiological and behavioral abnormalities that are

Author Manuscript Author Manuscript Author Manuscript Author Manuscript

remarkably similar to those observed in people with PTSD including a robust fear-conditioned memory of the trauma exposure, increased anxiety, exaggerated startle response, impaired memory for new information, enhanced negative feedback of the hypothalamic-pituitary-adrenal axis, decreased basal corticosterone, and increased hormonal and cardiovascular reactivity to an acute stressor (Zoladz et al., 2008; Zoladz et al., 2012; Zoladz et al., 2013; Zoladz et al., 2015). Some of these changes are reversed by drugs such as sertraline, clonidine, and tianeptine that have efficacy in the treatment of patients who have PTSD (Wilson et al., 2014a; Zoladz et al., 2013).

Multiple studies have demonstrated an increased risk of myocardial infarction and other cardiovascular disorders in people with PTSD (Ahmadi et al., 2011; Beristianos et al., 2016; Khazaie et al., 2013; Vaccarino et al., 2013). We previously reported that rats exposed to predator stress develop myocardial hypersensitivity to ischemic injury. (Rorabaugh et al., 2015; Rorabaugh et al., 2018) The goal of the present study was to use this stress model to characterize changes in myocardial histology and gene expression that may make the heart more vulnerable to myocardial infarction and other cardiac disorders. Our data provide evidence that predator-based psychosocial stress induces the formation of cardiac lesions characterized by necrosis, collagen deposition, infiltration of immune cells, and changes in gene expression that are indicative of cardiac tissue remodeling. These stress-induced changes may underlie the increased risk of cardiac disorders associated with PTSD and other chronic stress disorders.

Methods

Animals.

Male Sprague-Dawley rats (6-7 weeks of age at the beginning of the study) from an established breeding colony at Ohio Northern University were used for all experiments. The rat colony originated from Sprague-Dawley rats obtained from Charles River Laboratories (Boston, MA; Strain Code 001). The rats were housed on a 12-h light/dark cycle (lights on at 0700) in standard Plexiglas cages (two per cage) with free access to food and water. The animals originated from 4 different litters. Siblings were divided between stressed and nonstressed experimental groups to avoid the potential for litter bias. All procedures were approved by the Institutional Animal Care and Use Committee and were performed in compliance with the recommendations published in the 8th edition of *The Guide for the Care and Use of Laboratory Animals*.

Psychosocial Stress Procedure.

Rats were randomly assigned to “psychosocial stress” or “no stress” experimental groups. The stress regimen has been previously described and validated by multiple laboratories (Rorabaugh et al., 2015; Zoladz et al., 2008; Zoladz et al., 2013; Zoladz et al., 2015). Rats in the psychosocial stress group were given two acute stress sessions (exposure to a cat), which were separated by 10 days. The first stress session took place during the light cycle (between 0800 and 1300), and the second stress session took place during the dark cycle (between 1900 and 2100) so that the animals could not predict when they might re-experience the predator exposure.

Author Manuscript Author Manuscript Author Manuscript Author Manuscript

On Day 1, rats in the psychosocial stress groups were immobilized in plastic DecapiCones (Braintree Scientific; Braintree, MA) and placed in a perforated wedge-shaped Plexiglas enclosure (Braintree Scientific; Braintree, MA; 20 × 20 × 8 cm). This enclosure was then taken to a cat housing room and placed in a metal cage (61 × 53 × 51 cm) with an adult female cat for 1 h. The Plexiglas enclosure prevented any contact between the cat and rats, but the rats were still exposed to all non-tactile sensory stimuli associated with the cat. Canned cat food was smeared on top of the enclosure to direct the cat's attention toward the rats. An hour later, the rats were returned to their home cages. Rats in the no stress groups remained in their home cages during the 1-h stress period.

Social Stress.

Rats in the psychosocial stress groups were exposed to unstable housing conditions starting on the day of the first cat exposure (Day 1) and continuing throughout the paradigm until behavioral testing (Day 32). Rats in the psychosocial stress group were housed two animals per cage, but every day their cage mates were changed. Therefore, no rats in the psychosocial stress groups had the same cage mate on two consecutive days during the 31-day stress period. Rats in the no stress groups were also housed two animals per cage. However, nonstressed animals were cohoused with the same cage mate throughout the experiment. Nonstressed animals were handled daily to control for handling effects on stressed animals.

Behavioral Testing.

Three weeks following the second stress session (Day 32), rats were tested on the elevated plus maze (EPM) to assess anxiety-like behavior. Rats were placed on the EPM for 5 min, and their behavior was videotaped by a JVC hard disk camera hanging above the EPM and scored offline by two separate investigators who were blind to the experimental conditions of the animals. Time spent in the open arms of the maze was used as a measure of anxiety, and the total number of closed arm entries was used to assess locomotor activity.

RNA-sequencing.

Stressed and nonstressed rats (5 animals / group) were anesthetized with sodium pentobarbital (100 mg/kg ip), and hearts were quickly isolated and perfused for 5 minutes on a Langendorff isolated heart system to flush blood from the tissue. The left ventricle was immediately flash frozen in liquid nitrogen and stored at −80°C until it was used for RNA isolation. Total RNA was isolated using TRIzol reagent (Fisher Scientific Catalog # 15596026) according to the manufacturer's instructions. RNA was DNase I digested with a Turbo DNA-Free kit from Fisher Scientific (Catalog # AM1907) according to the manufacturer's protocol. The RNA was shipped on dry ice to the Michigan State University Research Technology Support Facility Genomics Core (East Lansing, MI). The RNA from each rat was quantified using a Quibit dsDNA High Sensitivity Assay (Thermo Fisher Cat #Q32851) and analyzed on an Agilent 2100 Bioanalyzer RNA Pico Chip. RNA sequencing libraries were made from each rat heart using the Illumina TruSeq Stranded mRNA library preparation kit. Equimolar amounts of libraries were pooled for multiplexed sequencing on a single Illumina NextSeq 500 lane in a 75 base pair single end format. Sequencing data were demultiplexed and converted to FastQ format.

Author Manuscript Author Manuscript Author Manuscript Author Manuscript

Raw Fastq files underwent quality control processing with FastQC (Andrews, 2010) software and were further processed with TrimGalore (Andrews, 2012) to remove low quality bases and to trim adapter sequences. Reads passing quality controls were aligned to the Rn6 version of the rat genome using STAR aligner software.(Dobin et al., 2013) Gene count files on the reverse strand were generated from alignment files with FeatureCounts (Liao et al., 2014) software using the RNor_6.0 ENSEMBL genome assembly. Differential gene expression analysis was produced in R (v3.3.3) software with the DESeq2 package (Love et al., 2014). Adjusted p-values (false discovery rate) were calculated in DESeq2 using the Benjamini-Hochberg equation (Benjamini Y and Y, 1995). Log_2-transformed, median-centered gene expression and genes within the defined gene ontology families were selected for heatmap generation using 'pheatmap' package in R. Volcano plots to visualize transcriptional changes were produced with GraphPad 7 software. Genes considered significant (adjusted p value < 0.05) were analyzed by gene ontology in R with 'ClusterProfiler' software (Yu et al., 2012).

Data availability statement.

Raw data from next-generation sequencing experiments were deposited in the National Center for Biotechnology Information Sequence Read Archive and are available under BioProject ID number PRJNA498684. Differential gene expression analysis of these data is shown at https://figshare.com/s/5f32d3c03635c9bf46f5.

Western Blots.

Frozen ventricular tissue (from the same rats described above for RNA sequencing) was used for western blotting with antibodies for alpha smooth muscle actin (Cell Signaling Technology, Danvers, MA; Catalog #19245), T-cadherin (Abcam, Cambridge, MA; Cat #ab167407), and glyceraldehyde-3-phosphate dehydrogenase (GAPDH) (Cell Signaling Technology, Danvers, MA; Catalog #2118). Alpha smooth muscle actin and T-cadherin bands were normalized to those of GAPDH.

Histology.

Stressed and nonstressed rats (6 animals / group) were euthanized with sodium pentobarbital (100 mg / kg, i.p.) followed by opening of the chest cavity. Hearts were removed, immersed in 10% neutral buffered formalin, and submitted to the Comparative Pathology and Mouse Phenotyping Shared Resource at The Ohio State University for tissue trimming, processing, and staining. Hearts were trimmed by longitudinal bisection perpendicular to the plane of the interventricular septum (Berridge et al., 2016). Two 5-μm thick sections of paraffin-embedded heart tissue were stained with hematoxylin and eosin (H&E) or Masson's trichrome stains and evaluated microscopically by a board certified veterinary pathologist who was blinded to treatment groups. Histology slides were digitally scanned at Charles River Laboratories in Spencerville, Ohio using a Leica ScanScope XT scanner at 20x magnification and Aperio ImageScope [v12.3.0.5056] viewing software. Microscopic evaluation included scoring of the following criteria on a scale of 1 to 10 where 1 represented no visible lesions and 2 through 10 represented ascending levels of severity of myofiber necrosis (1-10), mononuclear cell infiltrate (1-10), or fibrosis (1-10).

Author Manuscript Author Manuscript Author Manuscript Author Manuscript

Hearts from stressed and nonstressed rats (6 animals / group) were analyzed by immunohistochemistry using a CD31-specific antibody (Abcam, Cambridge, MA; Catalog # ab-28364). Five randomly chosen regions of the stained ventricular myocardium were photographed at 400 X magnification and the number of CD31 positive cells in each field was averaged to determine the number of CD31 cells for each heart. This process was repeated for each heart by 3 independent investigators who were blinded to treatment groups. The mean value of the three investigators was used to represent the number of CD31 positive cells for each heart.

Statistical Analyses.

Data are presented as the mean ± S.E.M. The unpaired Student's t test was used to compare data from stressed and nonstressed experimental groups in the elevated plus maze, western blots, histology, and immunohistochemistry. These analyses were performed using Graphpad Prism 7 software. P values < 0.05 were regarded as statistically significant. P values for normalized counts from RNA sequencing were adjusted using R (v3.3.3) software with DESeq2 as previously described (Love et al., 2014) (Benjamini Y and Y, 1995) to minimize the frequency of false discovery. Adjusted P values < 0.05 were regarded as statistically significant.

Results

Anxiety-related behavior in the elevated plus maze.

Previous work demonstrated that rats subjected to this stress model display anxiety-related behavior in the elevated plus maze (Rorabaugh et al., 2015; Zoladz et al., 2008; Zoladz et al., 2013). Consistent with previous studies, rats exposed to 31 days of psychosocial stress ($n = 11$) spent significantly ($t(21) = 9.13$, $p < 0.0001$) less time than nonstressed rats ($n = 12$) in the open arms of the maze (Fig. 1A). The number of closed arm entries was similar ($p = 0.47$) for stressed and nonstressed rats (Fig. 1B), indicating that stress had no significant effect on overall locomotor activity. These data provide behavioral validation of the efficacy of the stress regimen in rats that were subsequently used for cardiac analyses. Data from one stressed rat was excluded because the amount of time that it spent in the open arms of the elevated plus maze was more than 5 standard deviations from the mean.

Body weight.

Body weights of control and stressed rats were similar on day 1 of the stress protocol (278 ± 19 g and 290 ± 14 g for control and stressed animals, respectively; $p = 0.61$), and both experimental groups gained similar amounts of weight over the course of the 31-day stress regimen (187 ± 12 g and 185 ± 9 g; $p = 0.92$).

Stress-induced changes in cardiac gene expression.

RNA sequencing analysis was performed using RNA isolated from the left ventricular tissue from 5 stressed and 5 nonstressed rats. Principal component analysis (PCA) indicated that ventricles from nonstressed rats had variable baseline gene expression patterns that separated on principal component 1 (PC1), while ventricular tissue from all 5 stressed rats clustered

Author Manuscript Author Manuscript Author Manuscript Author Manuscript

closely and were separated by principal component 2 (PC2). (Fig. 2A). These data indicate that stress induced distinct and reproducible transcriptional changes in rat ventricles.

In light of our finding that stressed hearts undergo transcriptional alterations, we next sought to define these transcriptional programs. Out of 12,218 detected genes, 481 genes were significantly (adjusted P-value < 0.05) upregulated and 660 genes were significantly downregulated (Fig. 2B; the differential gene expression analysis for the entire data set is available at https://figshare.com/s/5f32d3c03635c9bf46f5). Gene ontology analysis indicated that upregulated genes were primarily associated with angiogenesis (GO:0001525) and endothelial cell migration (GO:0043542) (Fig. 2C; Table 1), mesenchyme development (GO:0060485) and mesenchymal differentiation (GO:0048762) (Fig. 2C; Table 2), and extracellular matrix organization (GO:0030198) (Fig. 2C; Table 3). Interestingly, downregulated genes were only associated with one gene cluster (protein polyubiquitination; GO:0000209) (Fig. 2C), suggesting that only upregulated genes fall within defined biologically relevant processes. Additionally, we ranked genes in order from increasing to decreasing $\log_2$-fold expression changes in stressed hearts and performed gene set enrichment analysis (GSEA) to identify pathways associated with stress. We found that 'Endothelial to Mesenchymal Transition' was among the top enriched gene sets (Normalized Enrichment Score=1.26, P=0.03) (Fig 2D). Thus both analyses (gene ontology and gene set enrichment analysis) are consistent with increased formation of mesenchymal tissue. These data suggest that stressed hearts may have an increase in fibrotic tissue. Notably, many genes that were significantly upregulated have been associated with cardiac fibrosis, including PDGFB,(Gallini et al., 2016) TBX2,(Shirai et al., 2009) SPARC,(Vaughan et al., 2018) and ACTA2.(Teekakirikul et al., 2010; Zeisberg et al., 2007) (Figure 2E). Differential gene expression analysis data for the entire data set is available at https://figshare.com/s/5f32d3c03635c9bf46f5.

Stress-induced cardiac fibrosis and immune cell infiltration.

RNA sequencing indicated significant upregulation of genes involved in angiogenesis, cell migration, differentiation into mesenchymal tissue, and assembly /organization of extracellular matrix (Fig. 2; Tables 1 – 3). Thus, H&E and Masson's trichrome staining were used to determine whether these changes in gene expression reflected histological changes in the myocardium. Multifocal lesions characterized by myofiber necrosis (Fig. 3A), infiltration of mononuclear immune cells (Fig. 3B), and collagen deposition (Fig. 3C) were identified in the ventricular walls of all (n = 6) stressed rats. These lesions were absent from the hearts of all (n = 6) nonstressed rats with the exception of 1 animal that exhibited minor fibrosis (score = 2) without necrosis or mononuclear cell infiltration.

RNA sequencing and western blots indicated that α-smooth muscle actin was upregulated at both the mRNA transcript ($t(8) = 4.60$, $p < 0.005$) (Fig. 4A) and protein ($t(8) = 2.69$, $p < 0.05$) (Fig. 4B) levels in stressed heart. Increased expression of this myofibroblast marker is consistent with the observed deposition of collagen in stressed hearts (Fig. 3C) (van Putten et al., 2016). We also observed that T-cadherin (CDH13) was significantly upregulated at the mRNA transcript ($t(8) = 5.56$, $p < 0.0005$) (Fig. 4C) and protein ($t(8) = 4.80$, $p = 0.001$) (Fig. 4D) levels in hearts from stressed rats. These stress-induced changes are consistent

Author Manuscript Author Manuscript Author Manuscript Author Manuscript

with fibrosis and extracellular matrix remodeling (Asada et al., 2007; Frismantiene et al., 2014).

Impact of stress on CD31 Positive cells.

RNA sequencing indicated that hearts from stressed rats exhibited upregulation of genes involved in angiogenesis, blood vessel morphogenesis, and endothelial cell migration (Fig. 2). CD31 is commonly used as an endothelial marker (Lv et al., 2018; Tian et al., 2018; Wang et al., 2018). Thus, we compared the number of CD31 positive cells in high magnification (400 X) images of ventricles from stressed and nonstressed hearts. Immunohistochemistry indicated a significant ($t(10) = 2.43$, $p < 0.05$) decrease in the number of CD31 positive cells in ventricles from stressed rats compared to ventricles from nonstressed rats (Fig. 5).

Discussion

PTSD and other forms of chronic psychosocial stress are associated with an increased risk of cardiovascular abnormalities including hypertension, endothelial dysfunction, atherosclerosis, cardiac arrhythmias, and myocardial infarction (Ahmadi et al., 2011; Beristianos et al., 2016; Grenon et al., 2016; Khazaie et al., 2013; Vaccarino et al., 2013). We previously reported that rats exposed to the predator- stress model used in this study develop myocardial hypersensitivity to ischemic injury (Rorabaugh et al., 2015; Rorabaugh et al., 2018). The present work demonstrated that these animals also develop multifocal cardiac lesions characterized by myofiber necrosis, fibrosis, and infiltration by mononucleated immune cells (Fig. 3). This was accompanied by changes in gene expression associated with endothelial cell migration, mesenchymal development, and extracellular matrix organization (Fig. 2; Table 1, Table 2, Table 3). In addition, changes in the expression of markers for endothelial to mesenchymal transition were observed at both the mRNA (Fig. 2) and protein levels (Fig. 4, Fig. 5). These data provide evidence of cardiac stress and tissue remodeling in rats exposed to predator stress . These changes in histology and gene expression may underlie our previous observation that rats exposed to this model develop myocardial hypersensitivity to ischemic injury.(Rorabaugh et al., 2015; Rorabaugh et al., 2018)

Cho et al. previously used DNA microarray analysis to assess changes in gene expression in the mouse heart following 1-10 days of exposure to a social defeat model (Cho et al., 2014). Similar to the current study, these investigators identified changes in gene expression that were indicative of extracellular matrix remodeling, angiogenesis, and the formation of mesenchymal tissue. This prior work differed from the present study in fundamental ways including the species (mouse vs rat), stress model (stress induced by an aggressor mouse vs a predator), the duration of stress (1-10 days vs 31 days), and the method of assessing gene expression (DNA microarray vs RNA sequencing). Despite these differences, similar stress-induced changes in gene expression were observed, suggesting that increased expression of genes related to these ontologies represent a fundamental cardiac response to psychosocial stress.

Author Manuscript Author Manuscript Author Manuscript Author Manuscript

Rats exposed to the psychosocial stress model used in the current study exhibit significant increases in superoxide, peroxynitrite, and total reactive oxygen species in circulating blood, brain, and adrenal tissue (Ebenezer et al., 2016; Wilson et al., 2013). These animals also exhibit increased expression of pro-inflammatory cytokines (interleukin-1β and interleukin-18), decreased expression of anti-inflammatory cytokines (interleukin-10 and interleukin-4), and increased expression of the NALP3 inflammasome in the brain(Wilson et al., 2013). However, these proinflammatory markers have not previously been assessed in hearts of animals exposed to this model. RNA sequencing did not identify significant changes in the presence of mRNA transcripts encoding pro-inflammatory cytokines in the heart. However, the fact that hearts from stressed rats were infiltrated with mononucleated immune cells provides evidence that this form of stress produces an inflammatory response in the heart.

The gene expression profile, increased secretion of collagen, increased expression of α-smooth muscle actin, and the decrease in the number of CD31 positive cell are consistent with endothelial to mesenchymal transition in hearts from stressed rats. In addition to these phenotypic markers, stressed hearts also exhibited upregulation of genes (Zeb1, bone morphogenetic protein-4, notch 1, β-catenin) (Cho et al., 2018) that are known to mediate endothelial to mesenchymal transition (Table 1). However, we did not trace fibroblast lineage to determine whether stressed hearts contain an increase in the number of fibroblasts of endothelial origin. Thus, we cannot exclude the possibility that the decrease in endothelial cells and the increase in mesenchymal markers (collagen and α-smooth muscle actin) occurred independent of each other rather than through the process of endothelial to mesenchymal transition.

T-cadherin was upregulated in stressed hearts at both the mRNA transcript and protein levels. Previous work demonstrated that T-cadherin is involved in the organization of collagen fibrils in vitro (Frismantiene et al., 2014) and that it promotes remodeling of the vascular wall following vascular injury (Kudrjashova et al., 2002). Asada et al. (Asada et al., 2007) reported that T-cadherin was upregulated in a rat model of liver fibrosis. Thus, it is not surprising that T-cadherin was upregulated in the heart under conditions that promote collagen deposition and fibrosis. However, we are unaware of any previous studies in which T-cadherin has been associated with extracellular matrix remodeling or fibrosis in the heart. Further work is needed to better understand the role of T-cadherin in myocardial fibrosis.

The observed decrease in the number of CD31 positive cells in stressed hearts (Fig. 5) seemed contradictory to the outcome of gene ontology analysis (Fig. 2C) which suggested that stressed hearts exhibit a gene expression profile indicative of increased angiogenesis. However, it should be noted that there is overlap in the content of these gene clusters. Several genes that were significantly upregulated (FLNA, NRP2, BMP4, FGFR1, EFNA1) at the mRNA level are part of both the angiogenesis (Table 1) and mesenchyme development gene clusters (Table 2). We have performed western blots on ventricular homogenates from both stressed and nonstressed rats for a number of proteins that are associated with angiogenesis including endothelial nitric oxide synthase, vascular endothelial growth factor receptor 3, and vascular cell adhesion molecule 1 (data not shown) and found no stress-induced effect on the expression of these angiogenesis markers at the protein level. These

Author Manuscript Author Manuscript Author Manuscript Author Manuscript

data suggest that overlap between gene clusters may have caused gene ontology analysis to falsely identify myocardial angiogenesis as a stress-induced response in these animals.

PTSD is associated with an increased risk of developing cardiac disorders (Ahmadi et al., 2011; Beristianos et al., 2016; Khazaie et al., 2013; Vaccarino et al., 2013). The identification of pharmacotherapies that can prevent the development of cardiac disorders in patients with PTSD or other forms of chronic psychological stress would be of great clinical value. Increased sympathetic signaling is a hallmark feature of PTSD, and sympatholytics such as clonidine and propranolol have demonstrated efficacy in treating trauma-related nightmares, intrusive thoughts, and hyperarousal in some patients with PTSD. (Alao et al., 2012; Belkin and Schwartz, 2015; Boehnlein and Kinzie, 2007; Kinzie and Leung, 1989; Lindgren et al., 2013; Onder et al., 2006) Clonidine prevents the development of some of the PTSD-like physiological (increased systolic and diastolic blood pressure, tachycardia, and adrenal hypertrophy) and behavioral (anxiety in elevated plus maze and increased startle response) effects induced by this animal model.(Zoladz et al., 2013) However, neither clonidine or propranolol prevent the development of myocardial hypersensitivity to ischemia in this rat model,(Rorabaugh et al., 2018) indicating that this stress-induced effect is not the result of excessive sympathetic signaling. The current data suggest that anti-inflammatory agents or pharmacotherapies that inhibit endothelial to mesenchymal transition and the deposition of collagen may be more effective approaches to protecting the heart from the adverse effects of psychosocial stress.

In conclusion, our data indicate that predator stress promotes myocardial necrosis, collagen deposition, infiltration of immune cells and reprogramming of myocardial gene expression. These effects are consistent with the observation that animals exposed to this model develop myocardial hypersensitivity to ischemic injury (Rorabaugh et al., 2015; Rorabaugh et al., 2018). They are also consistent with previous work demonstrating that people who develop PTSD and other forms of chronic stress are at increased risk of developing cardiac disorders such as myocardial infarction and arrhythmias (Ahmadi et al., 2011; Beristianos et al., 2016; Khazaie et al., 2013; Vaccarino et al., 2013). This predator-based model of psychosocial stress may provide a useful tool to understand the mechanism by which PTSD impacts the heart and to identify therapeutic strategies to prevent the development of heart diseases in people who suffer from PTSD and other chronic stress disorders.

Acknowledgements

The authors thank Dr. Kevin Childs (Michigan State University Research Technology Support Facility Genomics Core) for help with the RNA sequencing experiments and Dr. Krista LePerle (The Ohio State University Comparative Pathology and Mouse Phenotyping core facility) for preparing hearts for histological analysis.

Funding: This work was supported by a grant from the National Heart Lung Blood Institute (R15HL132322) to BRR and a core grant from the National Cancer Institute (P30CA016058) to The Ohio State University Comparative Pathology and Mouse Phenotyping core facility.

References

Ahmadi N, Hajsadeghi F, Mirshkarlo HB, Budoff M, Yehuda R and Ebrahimi R (2011). Post-traumatic stress disorder, coronary atherosclerosis, and mortality. Am J Cardiol 108: 29–33. [PubMed: 21530936]

Author Manuscript Author Manuscript Author Manuscript Author Manuscript

Alao A, Selvarajah J and Razi S (2012). The use of clonidine in the treatment of nightmares among patients with co-morbid ptsd and traumatic brain injury. Int J Psychiatry Med 44: 165–9. [PubMed: 23413663]

Asada K, Yoshiji H, Noguchi R, Ikenaka Y, Kitade M, Kaji K, et al. (2007). Crosstalk between high-molecular-weight adiponectin and t-cadherin during liver fibrosis development in rats. Int J Mol Med 20: 725–9. [PubMed: 17912467]

Belkin MR and Schwartz TL (2015). Alpha-2 receptor agonists for the treatment of posttraumatic stress disorder. Drugs Context 4: 212286. [PubMed: 26322115]

Benjamini Y and Y H (1995). Controlling the false discovery rate: A practical and powerful approach to multiple testing. Journal of the Royal Statistical Society. Series B (Methodological) 57: 289–300.

Beristianos MH, Yaffe K, Cohen B and Byers AL (2016). Ptsd and risk of incident cardiovascular disease in aging veterans. Am J Geriatr Psychiatry 24: 192–200. [PubMed: 25555625]

Berridge BR, Mowat V, Nagai H, Nyska A, Okazaki Y, Clements PJ, et al. (2016). Non-proliferative and proliferative lesions of the cardiovascular system of the rat and mouse. J Toxicol Pathol 29: 1s–47s.

Blanchard DC, Griebel G and Blanchard RJ (2003). Conditioning and residual emotionality effects of predator stimuli: Some reflections on stress and emotion. Prog Neuropsychopharmacol Biol Psychiatry 27: 1177–85. [PubMed: 14659473]

Boehnlein JK and Kinzie JD (2007). Pharmacologic reduction of cns noradrenergic activity in ptsd: The case for clonidine and prazosin. J Psychiatr Pract 13: 72–8. [PubMed: 17414682]

Cho JG, Lee A, Chang W, Lee MS and Kim J (2018). Endothelial to mesenchymal transition represents a key link in the interaction between inflammation and endothelial dysfunction. Front Immunol 9: 294. [PubMed: 29515588]

Cho JH, Lee I, Hammamieh R, Wang K, Baxter D, Scherler K, et al. (2014). Molecular evidence of stress-induced acute heart injury in a mouse model simulating posttraumatic stress disorder. Proc Natl Acad Sci U S A 111: 3188–93. [PubMed: 24516145]

Dedert EA, Calhoun PS, Watkins LL, Sherwood A and Beckham JC (2010). Posttraumatic stress disorder, cardiovascular, and metabolic disease: A review of the evidence. Ann Behav Med 39: 61–78. [PubMed: 20174903]

Dobin A, Davis CA, Schlesinger F, Drenkow J, Zaleski C, Jha S, et al. (2013). Star: Ultrafast universal rna-seq aligner. Bioinformatics 29: 15–21. [PubMed: 23104886]

Ebenezer PJ, Wilson CB, Wilson LD, Nair AR and J F (2016). The anti-inflammatory effects of blueberries in an animal model of post-traumatic stress disorder (ptsd). PLoS One 11: e0160923. [PubMed: 27603014]

Ehlers A, Hackmann A, Steil R, Clohessy S, Wenninger K and Winter H (2002). The nature of intrusive memories after trauma: The warning signal hypothesis. Behav Res Ther 40: 995–1002. [PubMed: 12296496]

Ehlers A, Hackmann A and Michael T (2004). Intrusive re-experiencing in post-traumatic stress disorder: Phenomenology, theory, and therapy. Memory 12: 403–15. [PubMed: 15487537]

Frismantiene A, Pfaff D, Frachet A, Coen M, Joshi MB, Maslova K, et al. (2014). Regulation of contractile signaling and matrix remodeling by t-cadherin in vascular smooth muscle cells: Constitutive and insulin-dependent effects. Cell Signal 26: 1897–908. [PubMed: 24815187]

Gallini R, Lindblom P, Bondjers C, Betsholtz C and Andrae J (2016). Pdgf-a and pdgf-b induces cardiac fibrosis in transgenic mice. Exp Cell Res 349: 282–90. [PubMed: 27816607]

Grenon SM, Owens CD, Alley H, Perez S, Whooley MA, Neylan TC, et al. (2016). Posttraumatic stress disorder is associated with worse endothelial function among veterans. J Am Heart Assoc 5: e003010. [PubMed: 27009621]

Hubbard DT, Blanchard DC, Yang M, Markham CM, Gervacio A, Chun IL, et al. (2004). Development of defensive behavior and conditioning to cat odor in the rat. Physiol Behav 80: 525–30. [PubMed: 14741237]

Khazaie H, Saidi MR, Sepehry AA, Knight DC, Ahmadi M, Najafi F, et al. (2013). Abnormal ecg patterns in chronic post-war ptsd patients: A pilot study. Int J Behav Med 20: 1–6. [PubMed: 21960258]

Author Manuscript Author Manuscript Author Manuscript Author Manuscript

Kinzie JD and Leung P (1989). Clonidine in cambodian patients with posttraumatic stress disorder. J Nerv Ment Dis 177: 546–50. [PubMed: 2769247]

Kudrjashova E, Bashtrikov P, Bochkov V, Parfyonova Y, Tkachuk V, Antropova J, et al. (2002). Expression of adhesion molecule t-cadherin is increased during neointima formation in experimental restenosis. Histochem Cell Biol 118: 281–90. [PubMed: 12376824]

Liao Y, Smyth GK and Shi W (2014). Featurecounts: An efficient general purpose program for assigning sequence reads to genomic features. Bioinformatics 30: 923–30. [PubMed: 24227677]

Lindgren ME, Fagundes CP, Alfano CM, Povoski SP, Agnese DM, Arnold MW, et al. (2013). Beta-blockers may reduce intrusive thoughts in newly diagnosed cancer patients. Psychooncology 22: 1889–94. [PubMed: 23255459]

Love MI, Huber W and Anders S (2014). Moderated estimation of fold change and dispersion for rna-seq data with deseq2. Genome Biol 15: 550. [PubMed: 25516281]

Lv YX, Zhong S, Tang H, Luo B, Chen SJ, Chen L, et al. (2018). Vegf-a and vegf-b coordinate the arteriogenesis to repair the infarcted heart with vagus nerve stimulation. Cell Physiol Biochem 48: 433–49. [PubMed: 30016789]

Nemeroff CB, Bremner JD, Foa EB, Mayberg HS, North CS and Stein MB (2006). Posttraumatic stress disorder: A state-of-the-science review. J Psychiatr Res 40: 1–21. [PubMed: 16242154]

Onder E, Tural U and Aker T (2006). A comparative study of fluoxetine, moclobemide, and tianeptine in the treatment of posttraumatic stress disorder following an earthquake. Eur Psychiatry 21: 174–9. [PubMed: 15964747]

Pitman RK, Rasmusson AM, Koenen KC, Shin LM, Orr SP, Gilbertson MW, et al. (2012). Biological studies of post-traumatic stress disorder. Nat Rev Neurosci 13: 769–87. [PubMed: 23047775]

Reynolds M and Brewin CR (1999). Intrusive memories in depression and posttraumatic stress disorder. Behav Res Ther 37: 201–15. [PubMed: 10087639]

Rorabaugh BR, Krivenko A, Eisenmann ED, Bui AD, Seeley S, Fry ME, et al. (2015). Sex-dependent effects of chronic psychosocial stress on myocardial sensitivity to ischemic injury. Stress 18: 645–53. [PubMed: 26458179]

Rorabaugh BR, Bui AD, Seeley SL, Eisenmann ED, Rose RM, Johnson BL, et al. (2019). Myocardial hypersensitivity to ischemic injury is not reversed by clonidine or propranolol in a predator-based rat model of posttraumatic stress disorder. Prog Neuropsychopharmacol Biol Psychiatry 89:117–124. [PubMed: 30194949]

Shirai M, Imanaka-Yoshida K, Schneider MD, Schwartz RJ and Morisaki T (2009). T-box 2, a mediator of bmp-smad signaling, induced hyaluronan synthase 2 and tgfbeta2 expression and endocardial cushion formation. Proc Natl Acad Sci U S A 106: 18604–9. [PubMed: 19846762]

Teekakirikul P, Eminaga S, Toka O, Alcalai R, Wang L, Wakimoto H, et al. (2010). Cardiac fibrosis in mice with hypertrophic cardiomyopathy is mediated by non-myocyte proliferation and requires tgf-beta. J Clin Invest 120: 3520–9. [PubMed: 20811150]

Tian D, Zeng X, Wang W, Wang Z, Zhang Y and Wang Y (2019). Protective effect of rapamycin on endothelial-to-mesenchymal transition in huvecs through the notch signaling pathway. Vascul Pharmacol 113:20–26. [PubMed: 30336218]

Vaccarino V, Goldberg J, Rooks C, Shah AJ, Veledar E, Faber TL, et al. (2013). Post-traumatic stress disorder and incidence of coronary heart disease: A twin study. J Am Coll Cardiol 62: 970–8. [PubMed: 23810885]

van Putten S, Shafieyan Y and Hinz B (2016). Mechanical control of cardiac myofibroblasts. J Mol Cell Cardiol 93: 133–42. [PubMed: 26620422]

Vaughan L, Marley R, Miellet S and Hartley PS (2018). The impact of sparc on age-related cardiac dysfunction and fibrosis in drosophila. Exp Gerontol 109: 59–66. [PubMed: 29032244]

Wang W, Wang Z, Tian D, Zeng X, Liu Y, Fu Q, et al. (2018). Integrin beta3 mediates the endothelial-to-mesenchymal transition via the notch pathway. Cell Physiol Biochem 49: 985.

Wilson CB, McLaughlin LD, Nair A, Ebenezer PJ, Dange R and Francis J (2013). Inflammation and oxidative stress are elevated in the brain, blood, and adrenal glands during the progression of post-traumatic stress disorder in a predator exposure animal model. PLoS One 8: e76146. [PubMed: 24130763]

Author Manuscript Author Manuscript Author Manuscript Author Manuscript

Wilson CB, McLaughlin LD, Ebenezer PJ, Nair AR, Dange R, Harre JG, et al. (2014a). Differential effects of sertraline in a predator exposure animal model of post-traumatic stress disorder. Front Behav Neurosci 8: 256. [PubMed: 25126063]

Wilson CB, McLaughlin LD, Ebenezer PJ, Nair AR and Francis J (2014b). Valproic acid effects in the hippocampus and prefrontal cortex in an animal model of post-traumatic stress disorder. Behav Brain Res 268: 72–80. [PubMed: 24675160]

Yu G, Wang LG, Han Y and He QY (2012). Clusterprofiler: An r package for comparing biological themes among gene clusters. Omics 16: 284–7. [PubMed: 22455463]

Zeisberg EM, Tarnavski O, Zeisberg M, Dorfman AL, McMullen JR, Gustafsson E, et al. (2007). Endothelial-to-mesenchymal transition contributes to cardiac fibrosis. Nat Med 13: 952–61. [PubMed: 17660828]

Zen AL, Whooley MA, Zhao S and Cohen BE (2012). Post-traumatic stress disorder is associated with poor health behaviors: Findings from the heart and soul study. Health Psychol 31: 194–201. [PubMed: 22023435]

Zoladz PR, Conrad CD, Fleshner M and Diamond DM (2008). Acute episodes of predator exposure in conjunction with chronic social instability as an animal model of post-traumatic stress disorder. Stress 11: 259–81. [PubMed: 18574787]

Zoladz PR, Fleshner M and Diamond DM (2012). Psychosocial animal model of ptsd produces a long-lasting traumatic memory, an increase in general anxiety and ptsd-like glucocorticoid abnormalities. Psychoneuroendocrinology 37: 1531–45. [PubMed: 22421563]

Zoladz PR and Diamond DM (2013). Current status on behavioral and biological markers of ptsd: A search for clarity in a conflicting literature. Neurosci Biobehav Rev 37: 860–95. [PubMed: 23567521]

Zoladz PR, Fleshner M and Diamond DM (2013). Differential effectiveness of tianeptine, clonidine and amitriptyline in blocking traumatic memory expression, anxiety and hypertension in an animal model of ptsd. Prog Neuropsychopharmacol Biol Psychiatry 44: 1–16. [PubMed: 23318688]

Zoladz PR, Park CR, Fleshner M and Diamond DM (2015). Psychosocial predator-based animal model of ptsd produces physiological and behavioral sequelae and a traumatic memory four months following stress onset. Physiol Behav 147: 183–92. [PubMed: 25911267]

Author Manuscript Author Manuscript Author Manuscript Author Manuscript

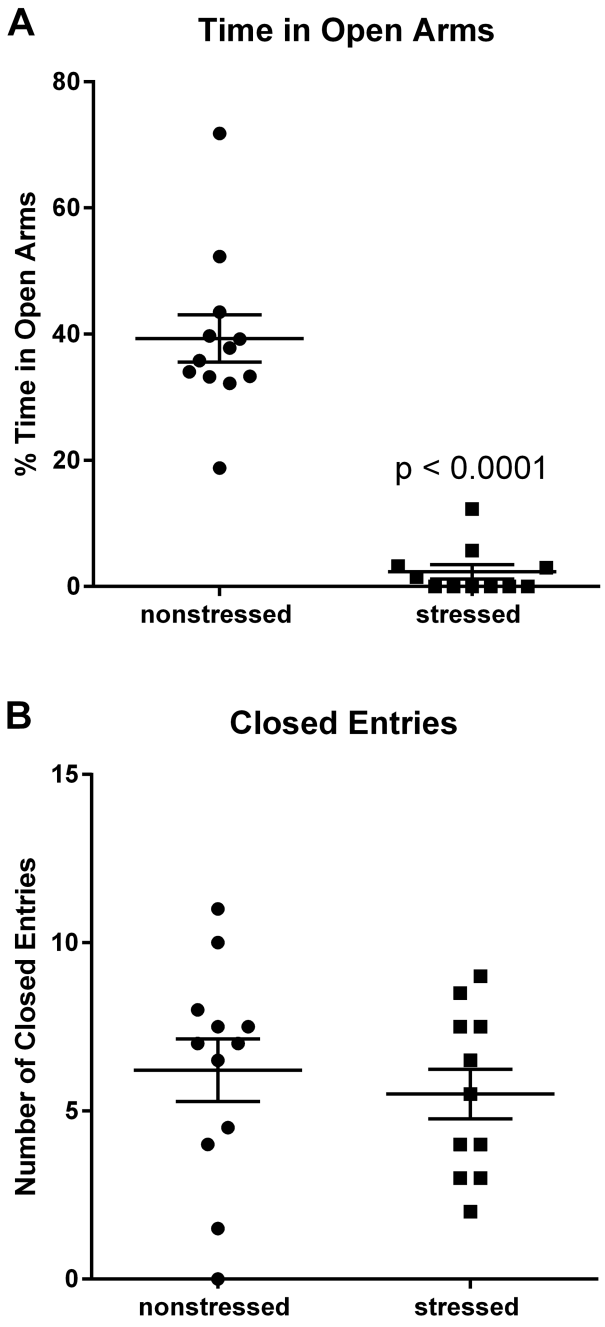

Fig. 1. Stressed rats exhibit anxiety-related behavior in the elevated plus maze.

Rats exposed to 31 days of psychosocial stress spent significantly less time than nonstressed rats in the open arms of the elevated plus maze (**A**). Stressed and nonstressed rats had similar numbers of entries into the closed arms, indicating that stress had no significant effect on locomotor activity (**B**). Data represent the mean ± S.E.M. of 11-12 animals per group.

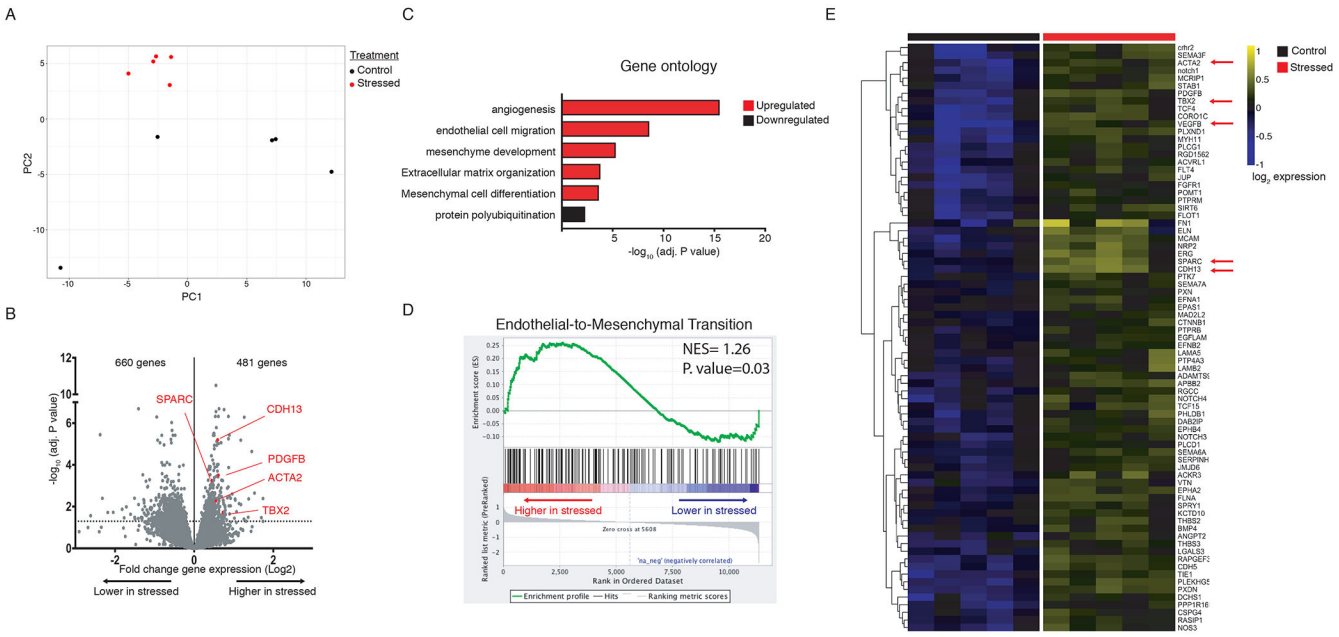

Fig. 2. RNA-sequencing of ventricular tissue from stressed and nonstressed rats.

Principal component analysis of gene expression profiles indicated that hearts from nonstressed rats have variable baseline gene expression that separated on principal component 1 (PC1), while hearts from all 5 stressed rats clustered closely and were separated by principal component 2 (PC2) (**A**). A volcano plot illustrating gene expression alterations and P values for 12,218 genes. Genes of interest are annotated in red (**B**). Gene ontology analysis identified significantly enriched gene family clusters for upregulated (red) or downregulated (black) genes (**C**). Genes were ranked in order of most to least enriched in stressed hearts and analyzed by Geneset Enrichment Analysis (GSEA). The enrichment plot shows the normalized enrichment score (NES) for genes associated with endothelial-to-mesenchymal transition (**D**). Heatmap showing median-centered, $\log_2$-fold changes for select upregulated genes identified from Gene Ontology families in panel C (**E**).

Author Manuscript Author Manuscript Author Manuscript Author Manuscript

Author Manuscript Author Manuscript Author Manuscript Author Manuscript

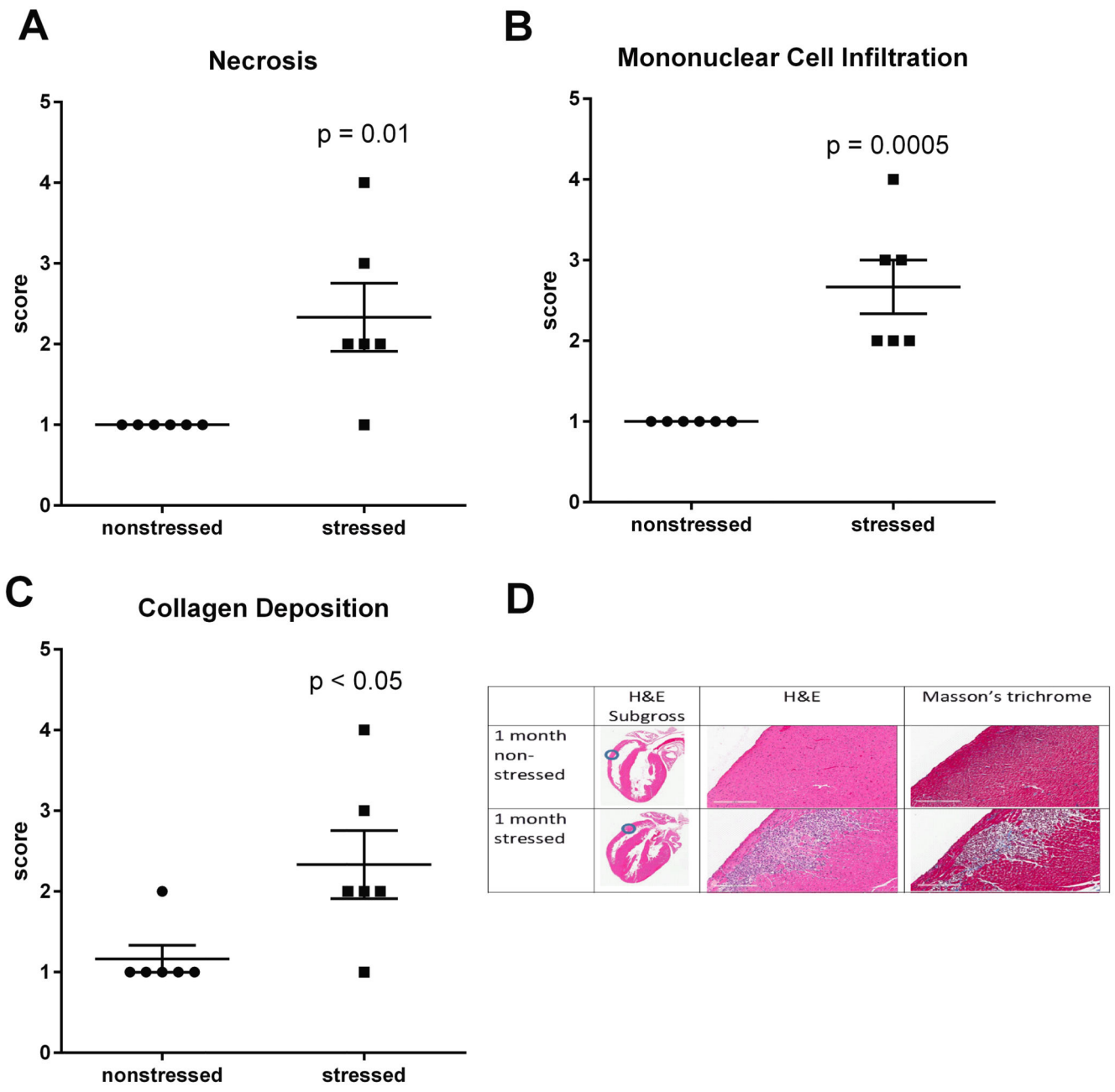

Fig. 3. Stress induces myocardial lesions characterized by fibrosis, necrosis, and mononuclear cell infiltration.

Hearts from stressed and nonstressed rats were evaluated by H&E and Masson's trichrome staining. Hearts from stressed rats developed multifocal lesions characterized by necrosis (**A,D**), infiltration by mononuclear immune cells (**B,D**), and collagen deposition (**C,D**). Data represent the mean ± S.E.M. of 6 animals. Representative photographs of heart sections are shown in panel **D**. Blue circles in photographs of subgross heart images indicate heart regions that were photographed at higher (15.8 X) magnification. Scale bars in panel D represent 200 μm.

Author Manuscript Author Manuscript Author Manuscript Author Manuscript

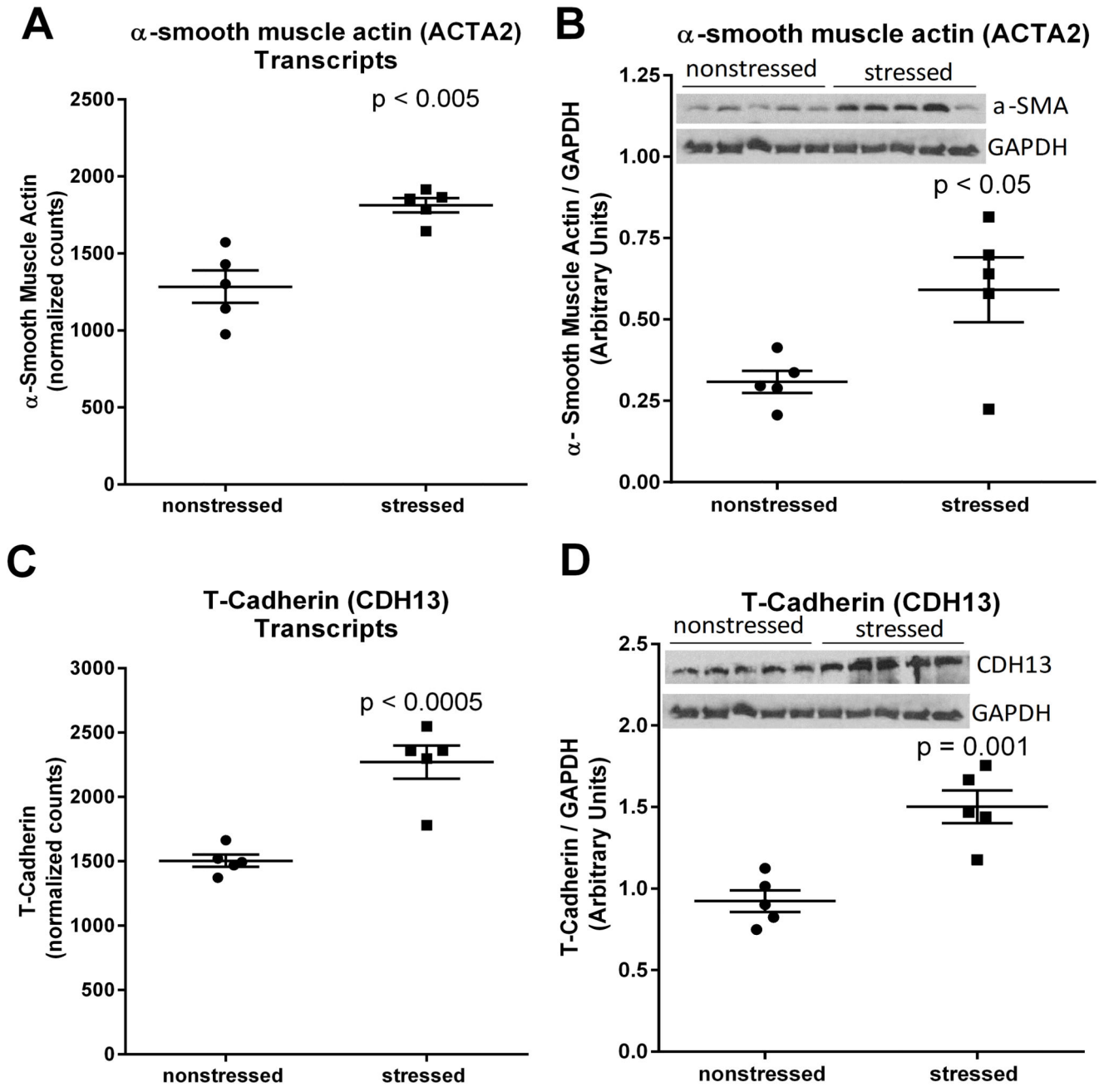

Fig. 4. Stress upregulates myocardial expression of α-smooth muscle actin and T-cadherin.

RNA sequencing identified upregulation of mRNA transcripts encoding α-smooth muscle actin (encoded by ACTA2) (**A**) and T-cadherin (encoded by CDH13) (**C**) in hearts from rats exposed to 31 days of psychosocial stress compared to hearts from nonstressed rats. Western blots confirmed significant increases in the expression of α-smooth muscle actin (**B**) and T-cadherin (**D**) at the protein level. Data in panels A and C represent the mean ± S.E.M. of 6 hearts. Data in panels **B** and **D** represent the mean ± S.E.M. of 5 hearts.

Author Manuscript Author Manuscript Author Manuscript Author Manuscript

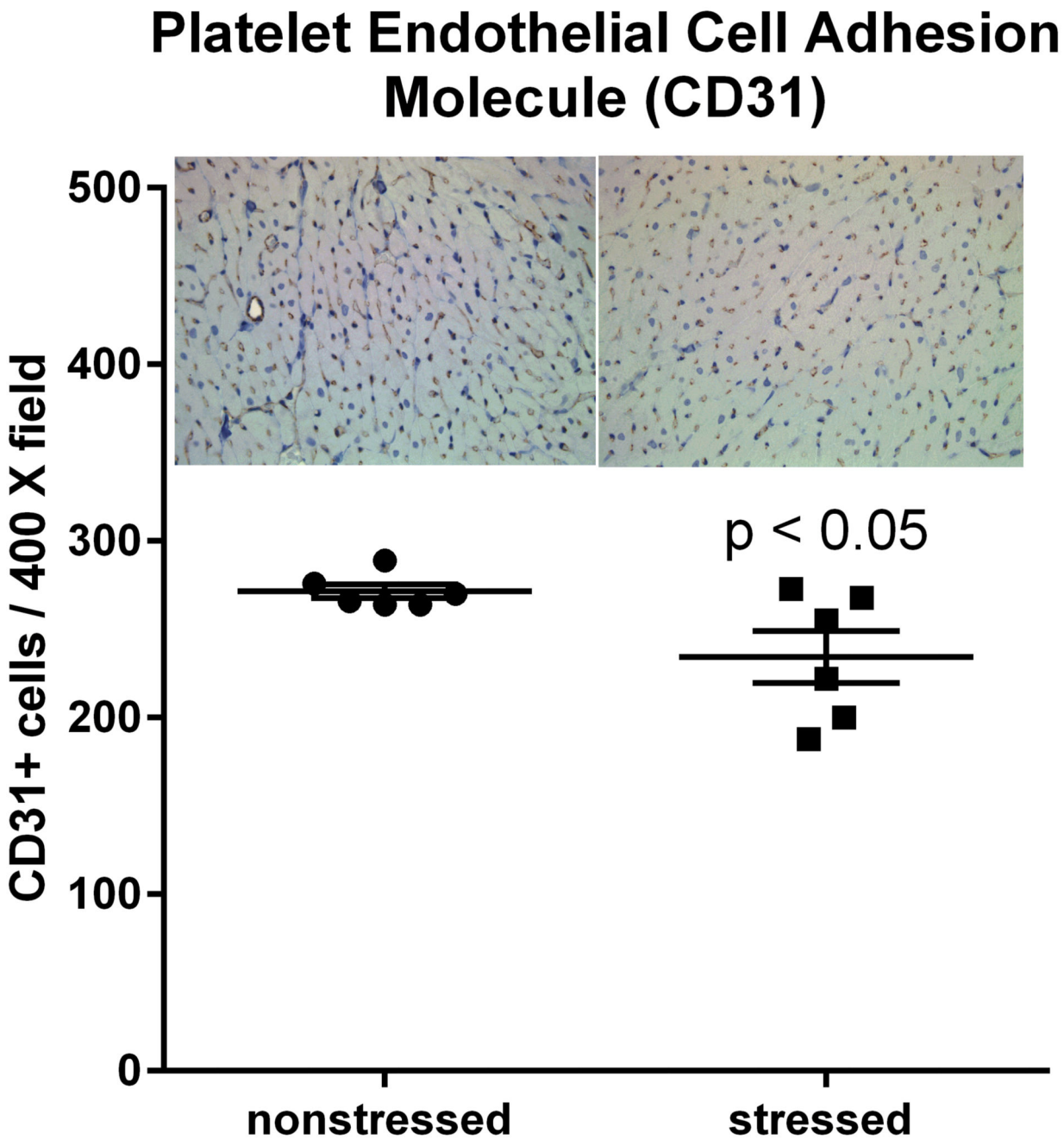

Fig. 5. Stressed hearts exhibit a decrease in the number of CD31 positive cells.

Predator-based psychosocial stress decreased the number of CD31-positive cells in the ventricular myocardium. Ventricular tissue was stained with a CD31-specific antibody, and the number of CD31 positive cells were counted by in 5 high (400 X) magnification fields for each heart by three independent investigators that were blinded to animal treatment. Data represent the mean ± S.E.M. of 6 hearts for each group.

Author Manuscript Author Manuscript Author Manuscript Author Manuscript

Table 1.

Selected changes in the number of mRNA transcripts (normalized counts) for genes in the angiogenesis (GO:0001525) and endothelial cell migration (GO:0043542) gene ontology clusters.

Gene Symbol	NCBI Reference #	Normalized Counts		Adjusted P value
		Nonstressed	Stressed	
RAPGEF3	NM_021690	1,597 ± 67	1,869 ± 93	1.64 E-06
PLXND1	NM_001107881	5,576 ± 340	8,524 ± 113	4.79 E-07
CDH13	NM_138889	1,504 ± 47	2,270 ± 129	6.34 E-06
TIE1	NM_053545	3,639 ± 192	4,347 ± 146	5.90E-05
FLT4	NM_053652	396 ± 38	605 ± 22	0.004
FLNA	NM_001134599	6,078 ± 176	7,931 ± 250	0.0001
NOS3	NM_021838	2,291 ± 122	3,078 ± 125	0.003
EPHA2	NM_001108977	198 ± 7	298 ± 12	0.0002
NOTCH1	NM_001105721	3,126 ± 194	4,405 ± 107	0.0002
NOTCH3	NM_020087	1,683 ± 102	2,104 ± 43	0.03
NOTCH4	NM_001002827	1,387 ± 94	1,869 ± 93	0.01
VEGFB	NM_053549	1,976 ± 245	3,329 ± 336	0.007
NRP2	NM_030869	2,305 ± 100	3,677 ± 261	0.0001
SPARC	NM_012656	44,383 ± 1,024	51,715 ± 11,878	0.0006
FGFR1	NM_024146	1,550 ± 130	2,121 ± 39	0.008
RASIP1	NM_001106261	1,113 ± 47	1,433 ± 42	0.004
PDGFB	NM_031524	693 ± 54	1,058 ± 40	0.0003
EFNA1	NM_053599	538 ± 12	657 ± 28	0.04
EFNB2	NM_001107328	1,351 ± 28	1,565 ± 28	0.03
PXN	NM_001012147	2,030 ± 50	2,364 ± 48	0.02
PTPRM	NM_001168632	2,625 ± 154	3,277 ± 33	0.02
ANGPT2	NM_134454	200 ± 21	284 ± 18	0.048
BMP4	NM_012827	164 ± 7	223 ± 14	0.03

Data represent the mean ± SEM of 5 hearts for each group.

Author Manuscript

Author Manuscript

Author Manuscript

Author Manuscript

Table 2.

Selected changes in the number of mRNA transcripts (normalized counts) for genes in the mesenchyme development (GO:0060485) and mesenchyme differentiation (GO:0048762) gene ontology clusters.

Gene Symbol	NCBI Reference #	Normalized Counts		Adjusted P value
		Nonstressed	Stressed	
ACTA2	NM_031004	1,285 ± 105	1,813 ± 47	0.004
FLNA	NM_001134599	6,079 ± 176	7,931 ± 250	0.0001
NRP2	NM_030869	2,305 ± 100	3,318 ± 180	0.0001
ERG	NM_133397	894 ± 41	1,284 ± 87	0.003
CORO1C	NM_001109327	1,449 ± 168	2,248 ± 89	0.005
DAB2IP	NM_138710	2,105 ± 101	2,714 ± 93	0.005
BMP4	NM_012827	164 ± 7	223 ± 14	0.03
SEMA7A	NM_001108153	1,631 ± 42	1,961 ± 45	0.009
SEMA5B	NM_001107091	66 ± 12	123 ± 8	0.02
SEMA3F	NM_001108185	432 ± 73	709 ± 29	0.02
TBX2	NM_001107033	147 ± 22	242 ± 12	0.02
NOTCH1	NM_001105721	3,126 ± 194	4,405 ± 107	0.0002
LAMA5	NM_001191609	2,083 ± 63	2,573 ± 140	0.03
PHLDB1	NM_001191578	7,833 ± 455	9,989 ± 504	0.03
FGFR1	NM_024146	1,550 ± 130	2,121 ± 39	0.008
EFNA1	NM_053599	538 ± 12	657 ± 28	0.04

Data represent the mean ± SEM of 5 hearts for each group.

Author Manuscript

Author Manuscript

Author Manuscript

Author Manuscript

Table 3.

Selected changes in the number of mRNA transcripts (normalized counts) for genes in the extracellular matrix assembly (GO:0085029) and extracellular matrix organization (GO:0030198) gene ontology clusters.

Gene Symbol	NCBI Reference #	Normalized Counts		Adjusted P value
		Nonstressed	Stressed	
MYH11	NM_001170600	2,117 ± 227	3,019 ± 103	0.02
ELN	NM_012722	1,799 ± 93	2,416 ± 199	0.03
PHLDB1	NM_001191578	7,833 ± 455	9,989 ± 504	0.03
PXDN	NM_001271261	3,835 ± 108	5,615 ± 134	3.22E-11
VTN	NM_019156	1,322 ± 87	1,746 ± 79	0.01
SERPINH1	NM_017173	7,703 ± 364	9,430 ± 234	0.02
FLOT1	NM_022701	2,132 ± 190	2,792 ± 60	0.03
LAMB2	NM_012974	19,323 ± 652	2,3729 ± 1440	0.04
THBS2	NM_001169138	1,253 ± 40	1,557 ± 75	0.02
ADAMTS9	NM_001107877	886 ± 41	1,174 ± 41	0.003
NOTCH1	NM_001105721	3,126 ± 194	4,405 ± 107	0.0002

Data represent the mean ± SEM of 5 hearts for each group.